Russian Journal of Earth Sciences, Vol. 22, ES4006
https://doi.org/10.2205/2022ES000805

Conjugate properties of Pi3/Ps6 pulsations according to Antarctica-Greenland observations

V. A. Martines-Bedenko[1], V. A. Pilipenko*[,1], M. Hartinger[2], and N. Partamies[3]

[1]*Schmidt Institute of Physics of the Earth, Moscow, Russia*
[2]*Space Science Institute, Boulder, Colorado, USA*
[3]*The University Centre in Svalbard, Longyearbyen, Norway*

Received 21 June 2021; accepted 21 July 2022; published 27 August 2022.

We consider interhemispheric properties of fine structure of substorm – quasi-periodic geomagnetic fluctuations, Pi3 pulsations, using data from conjugate magnetometers in Antarctica and Greenland. Pi3 pulsations are found to accompany both the substorm expansion/recovery phases and the steady magnetospheric convection (SMC) events. The epicenter of Pi3 power is located at the same latitude as maximal amplitude of magnetic bay. The interhemispheric properties of Pi3 pulsations are not consistent: in some events, coherent in-phase magnetic oscillations are observed in both hemispheres, in others, periodic variations are observed in one hemisphere only. When Pi3 pulsations are observed in both conjugate sites, their H-components are in-phase, which corresponds to the fundamental mode of field line oscillations between high-conductive ionospheres. Conjugate observations have provided an additional information on an elusive mechanism of Pi3 pulsations.

Keywords: Pi3 pulsations, conjugate observations, steady magnetospheric convection, Antarctica.

Citation: Martines-Bedenko, V. A., V. A. Pilipenko, M. Hartinger, and N. Partamies, (2022), Conjugate properties of Pi3/Ps6 pulsations according to Antarctica-Greenland observations, *Russian Journal of Earth Sciences*, Vol. 22, ES4006, doi: 10.2205/2022ES000805.

Introduction: Fine ULF structure of substorms and SMCs

Global responses of the magnetosphere and ionosphere to the solar wind/interplanetary magnetic field (SW/IMF) driving are revealed in different modes, comprising substorms, pseudo-substorms, and steady magnetospheric convection (SMC) events [*Partamies et al.*, 2009; *DeJong et al.*, 2007; *Milan et al.*, 2021].

Substorms are unloading events, which follow a period of open magnetic flux accumulation known as the growth phase. At onset (break-up), nightside reconnection of the magnetotail magnetic field lines dominates over dayside reconnection of IMF and magnetospheric field, so the accumulated magnetic energy is released in an explosive way.

SMCs (convection bays) are periods when the dayside and nightside reconnection rates are balanced, and quasi-steady convection dominates magnetospheric activity. The two-cell ionospheric current system caused by SMC is sustained by the transpolar voltage created by the motional electric field of the SW. During a SMC the magnitude of the magnetic disturbance is comparable to that of a substorm, but a SMC progresses to the expansion phase without a clear discontinuity, i.e., onset, like a substorm.

A pseudo-breakup is a phenomenon resembling a substorm but grouped in a different category. It displays a common morphology with a substorm until the onset, but it does not show a poleward expansion and terminates before changes propagate to the whole magnetosphere.

Magnetospheric modes are not laminar processes, but they are accompanied by an enhancement of magnetic field turbulence with various spatiotemporal scales. The occurrence of magnetospheric magnetohydrodynamic (MHD) resonators and waveguides acts as a natural band-pass amplifier in the ultra-low-frequency (ULF) band to a turbulent driving. Indeed, substorms reveal fine quasi-periodic structures in the Pi3 band, which cover periods of 5–20 min, beyond the nominal Pc5 band (150–600 s).

Pi3 pulsations have a particular importance for the fundamental space physics and its applications. These pulsations represent a quasi-periodic sequence of non-harmonic impulses. Due to steep wave fronts, the impulsive Pi3 pulsations induce the largest bursts of magnetic field variability (dB/dt) associated with geomagnetically induced currents (GICs) in electric power transmission lines (see references in review [*Pilipenko*, 2021].

*Corresponding author: pilipenko_va@mail.ru

Hence, the mesoscale turbulence within magnetospheric substorms is the dominant source of prolonged large dB/dt on the ground.

Pi3 pulsations are one of the few remaining ULF phenomena for which a physical mechanism has not been firmly established, despite numerous morphological studies. Probably, there are several possible mechanisms of quasi-periodic disturbances in the Pi3 band, though a criterion to discriminate them has not been found, namely:

- Sporadically occurring quasi-periodic variations of the SW/IMF parameters produce a planetary response inside the magnetosphere and on the ground, such as global Pi3 wave packet [*Han et al.*, 2007]. These global Pi3 oscillations are probably associated with magnetospheric cavity oscillations.
- Morphologically Pi3 pulsations with a dominant N-S component are like Ps6 pulsations with a dominant E-W component. Both have periods of 5–20 min and an amplitude of the magnetic field variation up to several hundred nT [*Solovyev et al.*, 1999]. Geomagnetic Ps6 pulsations are caused by localized vortex-like ionospheric structures [*Buchert et al.*, 1990]. The optical counterpart of strong Ps6 pulsations are omega bands, which occur in the early morning sector [*Saito*, 1978]. Ps6 pulsations tend to be observed in the narrow, less than 4° wide, latitude interval in the vicinity of the auroral electrojet. For brevity, we suppose that Ps6 pulsations are a sub-class of Pi3 pulsations.
- The morning/dusk flanks of the outer magnetosphere are regions with high-β plasma which is favorable for excitation of plasma instabilities. The injection of energetic electrons to the morning flank and hot protons to the dusk flank during substorms was found to be a trigger of long-period wave excitation [*James et al.*, 2013]. Magnetospheric pulsations driven by instability of the injected particles may contribute to Pi3 activity [*Vaivads et al.*, 2001].
- Consecutive Pi3 impulsive disturbances can be associated with quasi-periodic earthward fast plasma streams – bursty bulk flows (BBF) in the plasma sheet, expectedly driven by irregular magnetotail reconnection [*Keiling*, 2008].

Many traditional models of ULF wave physics where fundamental Alfvén field line oscillations are involved cannot be applied to Pi3 interpretation. For example, modeling of fundamental eigen oscillations at Gakona (Alaska) for quasi-dipole field line gave the estimate of ~5 mHz, which was much higher than the typical frequency of Pi3 pulsations observed at this station [*Guido et al.*, 2014].

Interhemispheric observations may provide additional clues to the physics of Pi3 pulsations. Such approach was fruitful for the study of drivers of Pc5 pulsations and ULF transients [*Pilipenko*, 2021]. Asymmetries in the magnetosphere-ionosphere system in geomagnetically conjugate regions are now receiving special attention and many focused studies. One of the overarching science question is: What are interhemispheric differences in substorm signatures and associated ULF wave activity, and what controls these differences? In this study we consider just one aspect of such global problem – conjugate properties of the fine structure of substorms – Pi3 pulsations. The unresolved questions for the ULF wave community are: How strongly substorm onsets and evolution are coupled with Pi3 pulsation excitation? Are Pi3 pulsations coherent in conjugate sites in the Northern and Southern hemispheres? Do Pi3 pulsations also accompany enhanced SMC? The solutions of these problems may help to approach the understanding of both substorm evolution and the physical mechanism of Pi3 pulsations. Our study is based on data from the conjugate Antarctica-Greenland magnetometer arrays.

Data analysis

Virginia Tech (http://mist.nianet.org/) deployed an autonomous adaptive low-power instrument platform (AAL-PIP) network of magnetometers with sampling cadence of 1 s in Antarctica [*Clauer et al.*, 2014]. Stations of this network are designed to be magnetically conjugate to the Greenland West Coast magnetometer chain (20 s cadence) along the 40° magnetic meridian operated by the Technical University of Denmark (https://www.space.dtu.dk). Figure 1 shows the locations of the AAL-PIP stations and the geomagnetic conjugate points of their counterparts in Greenland: PG0-UPN, PG1-UMQ, PG2-GDH, PG3-ATU, PG4-SKT, and PG5-GHB. Conjugate pair coordinates are given in Table 1. All stations are equipped with three-axes fluxgate magnetometers. The sensor axes are oriented along the local magnetic north (X), east (Y), and vertically down (Z).

The key starting problem in data analysis is to separate steep variations of the geomagnetic field during the substorm onset (magnetic bay) and superposed Pi3 pulsations. For that we have applied a high-pass filter with a cut-off time scale of 600–900 s (depending on event). The subtraction of the filtered variations from raw data provides detrended time series of Pi3 pulsations. The

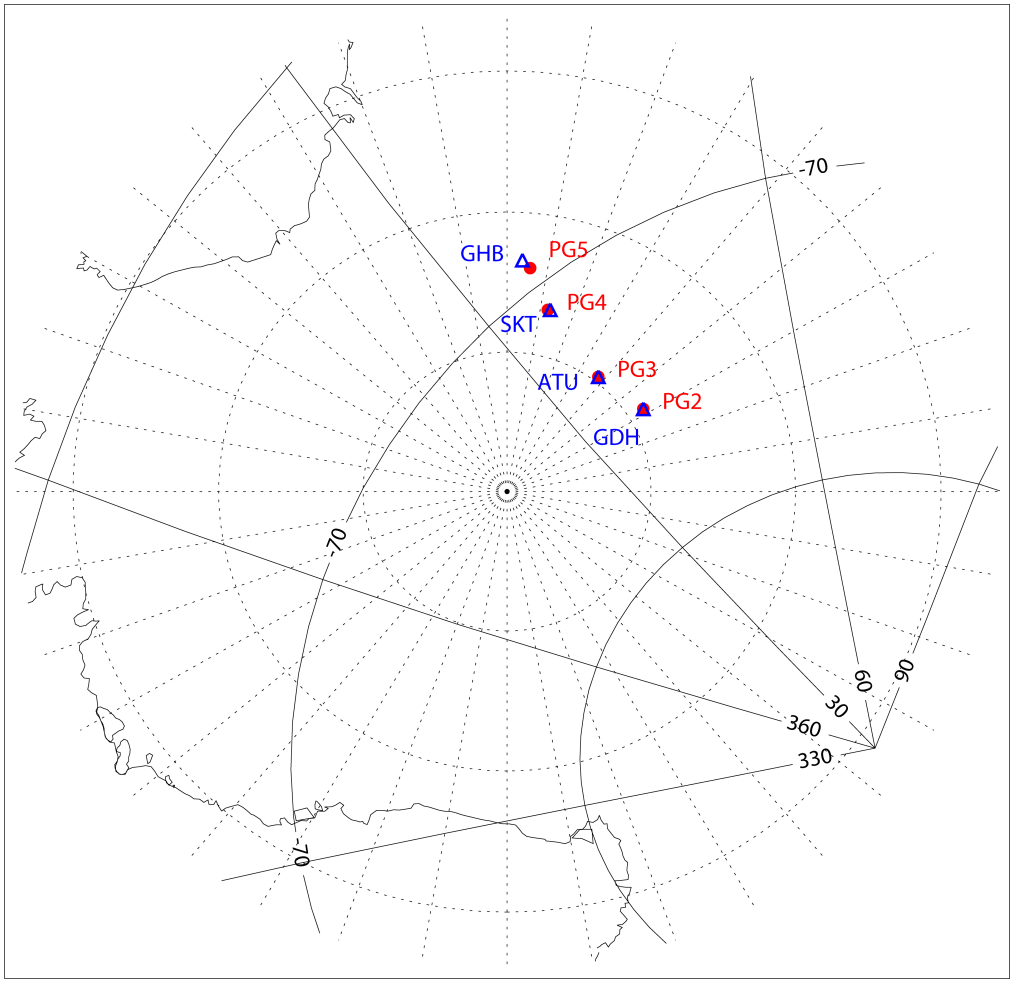

Figure 1: Map showing location of Antarctic stations and geomagnetic projection of the Greenland stations.

same technique has been used before to isolate Pi2 pulsations from the onset variations [*Martines-Bedenko et al.*, 2017]. Thus, upon data processing we have produced the following plots: stacked raw magnetograms of all 3 components; detrended magnetograms $X_d(t)$ which show ULF pulsations more clearly; and smoothed magnetograms (trend) $X_T(t)$ which describe the magnetic bay.

Further, with spectral analysis we have estimated the central frequency of the detrended Pi3 time series. The amplitude envelope $X_f(t)$ of Pi3 pulsations has been calculated with the use of the Hilbert transform of the band-filtered time series in the vicinity of this frequency.

The smoothed magnetic variations $X_T(t)$ and the amplitude envelope of the detrended ULF variations $X_f(t)$ have been used to construct contour maps in the geomagnetic latitude – time (Φ–UT) coordinates (magnetic keogram) [*Kozyreva et al.*, 2018]. Keograms demonstrate the time evolution of the latitudinal profile of disturbance under study. Thus, meridional chains of magnetometers in both hemispheres "scan" the development along the meridian of the latitudinal structure of the substorm and the Pi3 pulsation. The reference value of the magnetic field is its value before the substorm onset. The positive deviations ($\Delta X > 0$) are marked red, negative deviations ($\Delta X < 0$) are marked blue. Keograms for magnetic deflections

Table 1: Magnetometer Stations in Northern/Southern Hemisphere

Station	Geogr Lat	Geogr Lon	CGM Lat	CGM Lon
GDH	69.25°	306.47°	74.5°	37.8°
PG2	−84.42°	57.95°	−75.7°	39.1°
ATU	67.93°	306.43°	73.2°	36.8°
PG3	−84.81°	37.63°	−73.9°	36.7°
SKT	65.42°	307.10°	70.7°	36.1°
PG4	−83.34°	12.25°	−71.2°	36.4°
GHB	64.17°	308.27°	69.2°	36.8°
PG5	−81.96°	5.71°	−69.9°	37.2°

Corrected geomagnetic (CGM) coordinates were calculated for epoch 2016 (using http://sdnet.thayer.dartmouth.edu/aacgm/aacgm_calc.php#AACGM.

are shown as color plots, keograms for ULF amplitudes are shown as isolines to discriminate them more clearly.

To characterize the global space weather environment of the events under study we have used information on the SW/IMF parameters from the OMNI database and the geomagnetic indices. The standard IAGA auroral index *AE* (https://wdc.kugi.kyoto-u.ac.jp/aedir/) and provisional index SML from the SuperMAG portal (https://supermag.jhuapl.edu) have been used. Whenever possible, we use data of onboard magnetometer and energetic electron detector at GOES-15 (105° West) and GOES-13 (78° West) geosynchronous satellites, though these satellites are rathe far shifted longitudinally from the 40° meridian.

To discriminate substorms and non-substorm events we have used the community recognized substorm onset list, though all existing onset identification techniques have limitations. We have used a list of auroral substorm onsets as identified by the *Newell and Gjerloev* [2011] technique which is based on the SuperMAG derived auroral electrojet indices. As a measure of substorm activity we use the SML index. This index is analogous to the classical AL index but is calculated using data from 110 stations deposited on the SuperMAG portal. We have analyzed the period 2017–2018, however the available database has a limited seasonal coverage, because during winter months in Antarctica the automatic stations cannot operate.

Typical examples of Pi3 events during substorms

From 62 identified Pi3 events during the period 2017–2018 we present here the typical cases with most monochromatic variations. In these cases, the coherency between different stations can be examined most reliably.

Conjugate Pi3 pulsations

During the event on 2018/02/28, 0000–0130 UT, Pi3 pulsations are observed on the background of a weak substorm (Figure 2). The substorm is driven by IMF B_z<0 and triggered by a northward IMF turning. The *AE* index reaches ~180 nT, whereas SML index reaches about −300 nT.

The high-pass filtering makes it possible to separate the magnetic bay and ULF activity from the raw data (Figure 3).

This figure shows the stacked raw magnetograms of X component (upper panel); detrended magnetograms X_d which demonstrate ULF pulsations more clearly (middle panel); and smoothed magnetograms (trend) which describe the magnetic bay X_T (bottom panel). The green line denotes the Hilbert amplitude X_f at selected frequency 1.9 mHz. In Y –and Z – components pulsations are weaker and not shown.

The latitudinal profile of the spectral power in the band 1.8–1.9 mHz is shown in Figure 4. Maximal Pi3 activity within this spectral band is observed at $\Phi \sim 74°$ (ATU-PG3 pair). Pi3 variations are coherent in both hemispheres, at station pairs ATU-PG3 and PG5-GHB (Figure 3). At lower latitude (PG5) Pi3 pulsations are out-of-phase with pulsations at higher latitude (PG3).

The keograms of magnetic bay and Pi3 spectral power are shown in Figure 5. The keogram of the magnetic bay disturbances in the Northern hemisphere demonstrates poleward propagation. The maximum of Pi3 power is observed at the same latitude as the maximum of the magnetic bay in both hemispheres. Keograms have shown that the time-latitude structure of Pi3 intensity closely follow the leap-type poleward motion of magnetic bay. This observational fact may indicate that the excitation mechanism of Pi3 pulsations is closely associated with the intensification of the magnetosphere-ionosphere current system.

Non-conjugate Pi3 pulsations

The substorm on 2017/01/05, 0020–0100 UT, is associated with an IMF $B_z < 0$ condition. The *AE* index gradually increases up to ~ 600 nT, and SML to ~ −800 nT. During this substorm Pi3 pulsations in X-component with dominant $f \sim 2.0$ mHz are recorded at ATU, but no similar signatures can be seen at conjugate station PG4 (Figure 6). These pulsations (X-component) are superposed on the substorm magnetic bay. No Pi3 signatures can be seen at other nearby stations along the Antarctic profile. In Y – an Z – components pulsations are weaker and not shown.

An energetic electron injection is observed at GOES-15 at 0040 UT (not shown). The magnetic bay seen on the ground and the depression of magnetospheric magnetic field are similar, but ground Pi3 pulsations have no signature at geostationary orbit.

Alike the previous event, the similar procedure has been applied to isolate ULF fluctuations and background geomagnetic variations. Because Pi3 pulsations are observed only in one hemisphere, so the keograms are shown for this hemisphere only. Keograms of ULF power in the band 1.8–2.0 mHz show that the maximal Pi3 power in the Northern hemisphere is observed at the same latitude where the largest magnetic bay disturbance ΔB occurs (Figure 7).

This event may be considered as a typical example of non-conjugate Pi3 pulsations during a substorm.

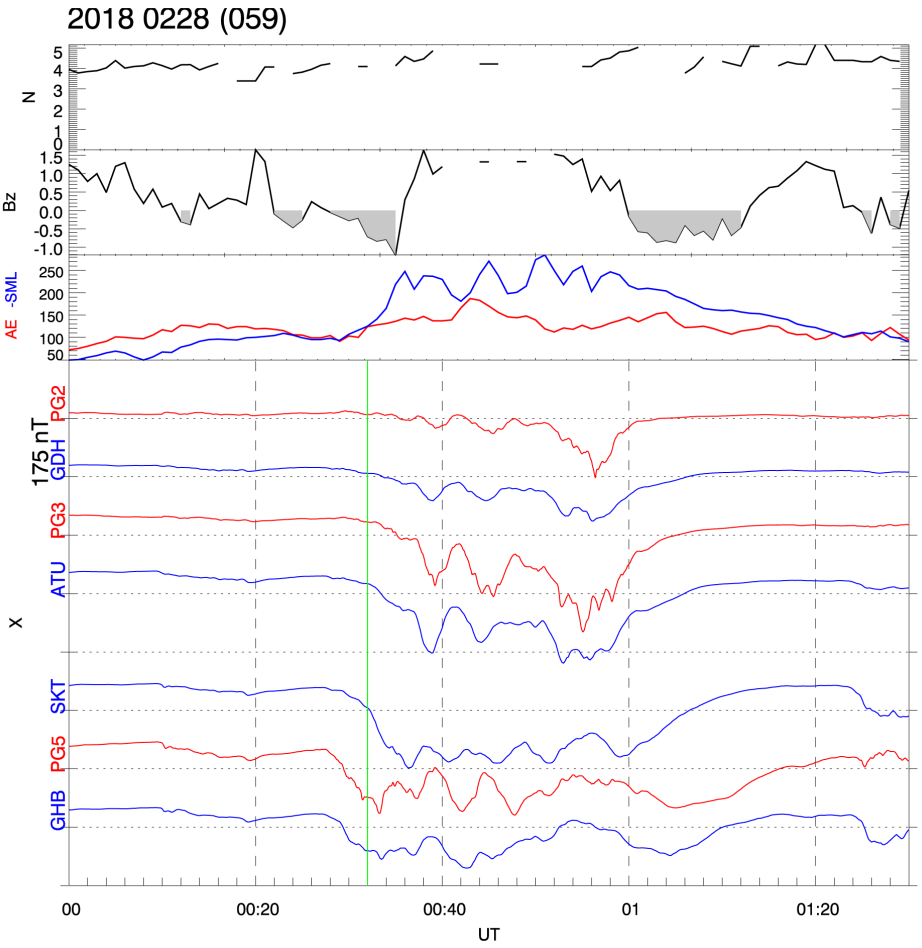

Figure 2: Magnetograms of the event on 2018/02/28, 0000-0130 UT (bottom panel). Upper panels show solar wind density N, IMF B_z component, and AE and reversed SML indices. The vertical green line indicates the substorm onset.

Typical example of Pi3 pulsations during SMC

These events are not included in the SuperMAG substorm list. Probably, they can be attributed to the SMC events.

Conjugate Pi3 event

The event on 2017/02/27, 0200–0340 UT, occurs during relatively low AE~20–40 nT, though IMF is southward, B_z<0 (Figure 8). At the same time, SML decreases to -140 nT. No electron injection is observed at both GOES satellites. Since 0220 UT irregular magnetic pulsations start at GOES, but their spectral content does not coincide with the one of ground Pi3 waves (not shown).

In this event one can see a possibility of good conjugacy of Pi3 pulsations between the Northern and Southern hemispheres. Quasi-periodic variations of X-component with dominant $f \sim 2.2$ mHz are in-phase and have comparable magnitudes at conjugate stations SKT-PG5. In the Y component the pulsation signatures are weaker.

However, the latitudinal profile of the ULF power (in the band 1.8–1.9 mHz) shows that their power peaks are latitudinally separated: in the Northern hemisphere it is at $\Phi \sim 71.5°$, whereas in the Southern hemisphere it is around 70.0° (Figure 9).

It seems, that the ULF conjugacy may deviate from the nominal conjugacy estimated with a geomagnetic field model. This feature will be discussed further.

The keograms show that the maximal Pi3 power is observed at the same latitude, where the largest magnetic bay disturbance ΔX occurs (Figure 10).

This event may be considered as an example of conjugate Pi3 pulsations during a SMC event.

Statistics of correlation between N/S variations during substorms

Here we provide some simple statistics on possible coherence between the fine structure of substorms in conjugate sites. The correlation coefficient R between X-components is calculated dur-

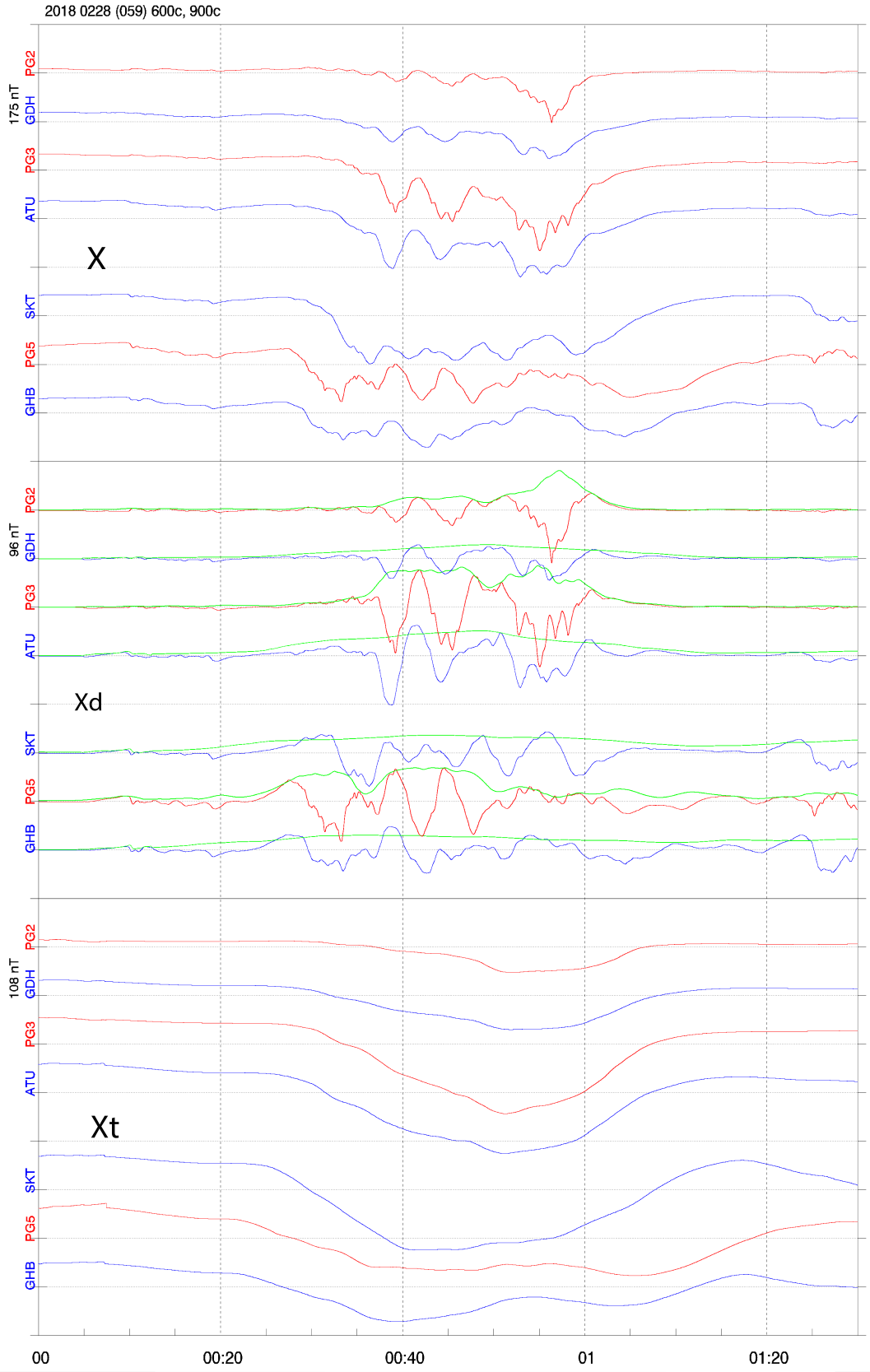

Figure 3: Raw magnetograms of X-component (upper panel), detrended ULF magnetograms (middle panel), and spline smoothed variations (bottom panel) for the event 2018/02/28, 0000-0130 UT. The Hilbert transform amplitude is shown as green line.

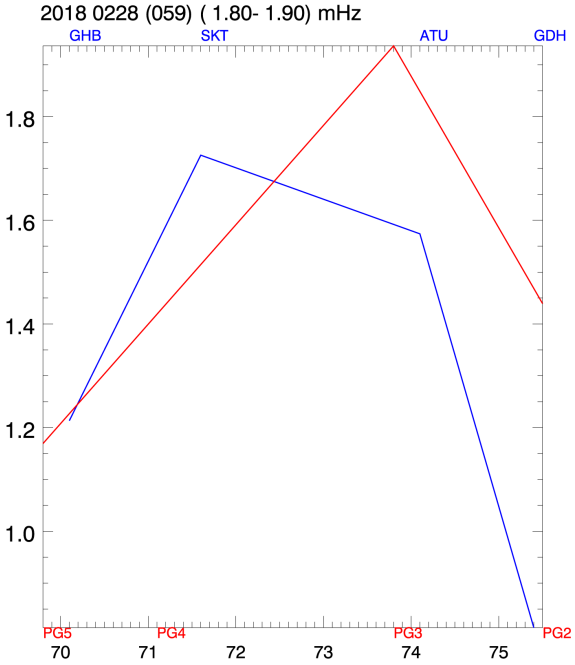

Figure 4: Latitudinal profile of the spectral power (X-component) in the band 1.8–1.9 mHz in both hemispheres for the event 2018/02/28, 0000-0130 UT

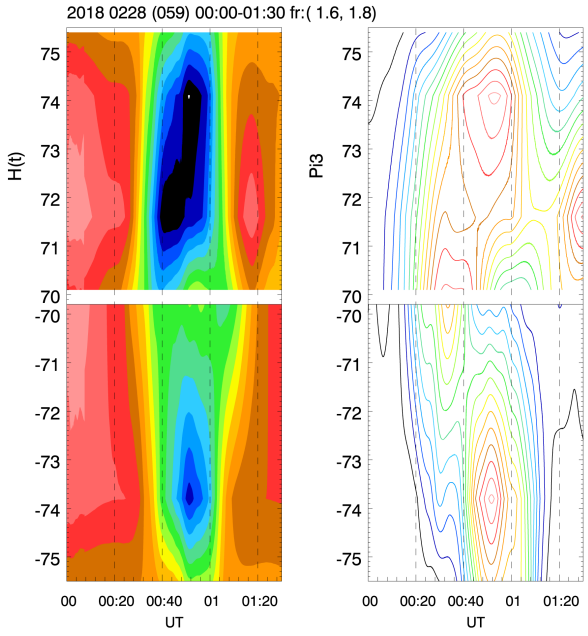

Figure 5: The keograms of magnetic disturbance (X-component) and Pi3 spectral power in Northern (upper panels) and Southern (bottom panels) hemispheres for the event 2018/02/28, 0000-0130 UT.

ing a 1-hour interval after substorm onset. The data for each time interval were first detrended by a subtraction of a 3-rd order polynomial. As a measure of Pi3 intensity we use the variance *VAR* of detrended magnetic variations. We have analyzed data for the year 2017. However, winter Antarctic months are missing because of the equipment "freezing". In the available conjugate data, we found 26 isolated substorms/SMSs with data at ATU-PG3 and SKT-PG4 pairs, and 19 events at GHB-PG5 pair.

The results for 3 pairs of Greenland-Antarctica stations are presented in Figure 11 as follows: *R*, magnetic field variance *VAR* at the Northern and Southern stations (in log-scale), and an absolute value of *SML* index. The *VAR* parameter, which is a proxy for the intensity of magnetic field variations, demonstrates a tendency to follow the |SML| magnitude at all stations. At ATU-PG3 and SKT-PG4 pairs the variance in the Northern hemisphere slightly exceeds that in the Southern hemisphere, whereas at GHB-PG5 variance is nearly the same in both hemispheres. Antarctic summer months predominantly contribute to the statistics, therefore nearly the same variances of magnetic fluctuations in both hemispheres indicate that asymmetry of the background ionospheric conductance is not significant for Pi3 intensity.

The correlation is not consistent. At all pairs, R varies between 0.1 and 0.8. At the ATU-PG3 pair, there are 11 events with $R > 0.6$, that is ~40% of recorded events. At SKT-PG4 pair, a good correlation, R>0.6, is observed for 7 events, which is ~27% of all events. At GHB-PG5 pair, 6 events with $R > 0.6$ are recorded, which constitutes ~31% of all events.

Field-aligned wave structure and phase relationships in conjugate points

The ground observation in conjugate sites makes it possible to determine the field-aligned structure (along coordinate s) of ULF disturbances in the magnetosphere. The relations of electric E and magnetic B components of Alfvénic disturbances with field line displacement ξ and with each other are predicted by MHD theory as follows

$$\frac{E_x}{B_0} = \partial_t \xi_y B_y = \partial_s (B_0 \xi_y) \partial_s E_x = -\partial_t B_y, \qquad (1)$$

in (1) s is the coordinate along a field line, X coordinate corresponds to the North-South direction, y is in the azimuthal (East-West) coordinate. Under high-conductive ionospheres, $\Sigma_P >> \Sigma_A$ (when the height-integrated Pedersen conductance Σ_P is higher than the Alfven wave conductance $\Sigma_A = (\mu_0 V_A)^{-1}$ determined by the magnetospheric Alfven velocity V_A), the Alfvén fundamental mode has a symmetric structure of $E(s)$ and $\xi(s)$ relative to the top of a field line with nodes in the ionospheres, and asymmetric structure of $B(s)$ (Figure 12).

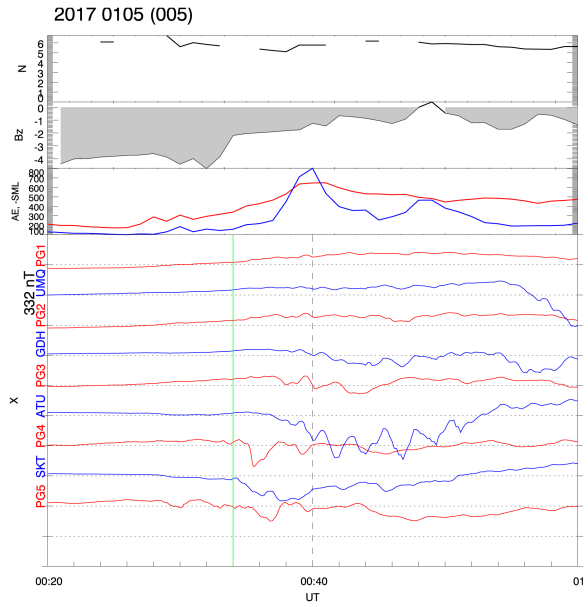

Figure 6: The event on 2017/01/05, 0020-0100 UT. The same format is in Fig. 2.

The magnetic ground disturbances in conjugate hemispheres (X-components) must be in-phase.

These relationships reverse under low-conductive ionospheres ($\Sigma_P << \Sigma_A$). The asymmetric $E(s)$ and $\xi(s)$ structure and symmetric $B(s)$ structure must produce an out-of-phase response on the ground in conjugate sites. The phase relationships between ground magnetic response in conjugate points are determined by the field-aligned structure of disturbance in the magnetosphere and are valid either resonant or forced oscillations.

Let us consider the properties of field-aligned current (FAC) $j_{\|}$ in conjugate points transported by an Alfvénic disturbance. From Ampere's relationship (here Rot is 2D operator transverse to $\mathbf{B}_0$)

$$j_{\|} = \mu_0^{-1} Rot B. \quad (2)$$

From (2) it follows that the FAC structure $j_{\|}(s)$ is the same as that of $B(s)$. Therefore, for a mode between high-conductive ionospheres with an asymmetric distribution of $B(s)$ in respect to the top of a field line, FACs in both hemispheres are simultaneously flowing in/out of conjugate ionospheres (Figure 12). For the even mode, FACs flow into one ionosphere and outwards the other. For the low-conductive ionospheres, for the mode with an anti-node of $B(s)$ at the equatorial plane the FAC is outflowing one hemisphere, and inflowing the other.

In our events when Pi3 oscillations have been observed in both hemispheres, their X-components were in-phase. Thus, the possibility of the even $B(s)$ mode structure as an origin of Pi3 pulsations must be rejected. Despite night-time conditions, the observed in-phase relationships in conjugate points indicate the symmetric (fixed end) oscillations between high-conductive ionospheres. Probably, sufficiently high conductance of the ionosphere is produced by elevated electron precipitation during substorms.

Discussion

The substorm onset and evolution are closely associated with ULF signatures: Pi1 bursts (0.1–1 Hz), Pi2 train (~8–10 mHz), and Pi3/Ps6 (~1–4 mHz) pulsations. Both polar and auroral substorms are accompanied by irregular Pi3 geomagnetic pulsations [*Kleimenova et al.*, 2012]. There is still no clear understanding of the magnetospheric counterpart of Pi3 pulsations. Are they a result of some quasi-periodic driving by the SW/IMF parameters, or some self-excited/triggered wave process in the night side magnetosphere?

The ULF periodicity may be determined by a resonant response of the nightside magnetosphere to irregular driving in the magnetotail. The Pi3 frequencies may correspond to eigenfrequency of some coupled magnetosphere–ionosphere system with a low quality factor Q. However, the physics of this system remains unknown. Traditionally, ULF wave processes are interpreted as a fast mode magnetospheric cavity resonance or field line Alfvén oscillations.

Like mid-latitude Pi2 pulsations can result from a plasmaspheric cavity resonance, Pi3 pulsations may be associated with some MHD cavity response [*Cheng et al.*, 2014]. For example, a MHD cavity resonator may be formed in a nightside region with decreased Alfvén velocity [*Leonovich and Mazur*, 2005]. However, localized ground responses (2°) and low coherence between ground and space pulsations indicate that Pi3 cannot be associated with large-scale cavity oscillations.

In favor of the Alfvén-wave mechanism, one may recollect the satellite observations of waves with periods > 10 min, that are beyond the classical Pc5 band. Strong compressional pulsations in the Pi3 and were observed in the outer magnetosphere ($L > 8$) in the morning and afternoon sectors [*Vaivads et al.*, 2001]. They were polarized close to the meridian plane with comparable compressional and transverse components. The typical azimuthal size corresponded to the wave number m~15–70, whereas the radial scale size usually was larger than the azimuthal. Such polarization structure corresponds to Alfvénic poloidal mode (or ballooning mode) in a finite-β plasma [*Mazur et al.*, 2014]. The pulsations were propagating in the sunward direction and were often related to substorm activity. Also, Pi3 waves with

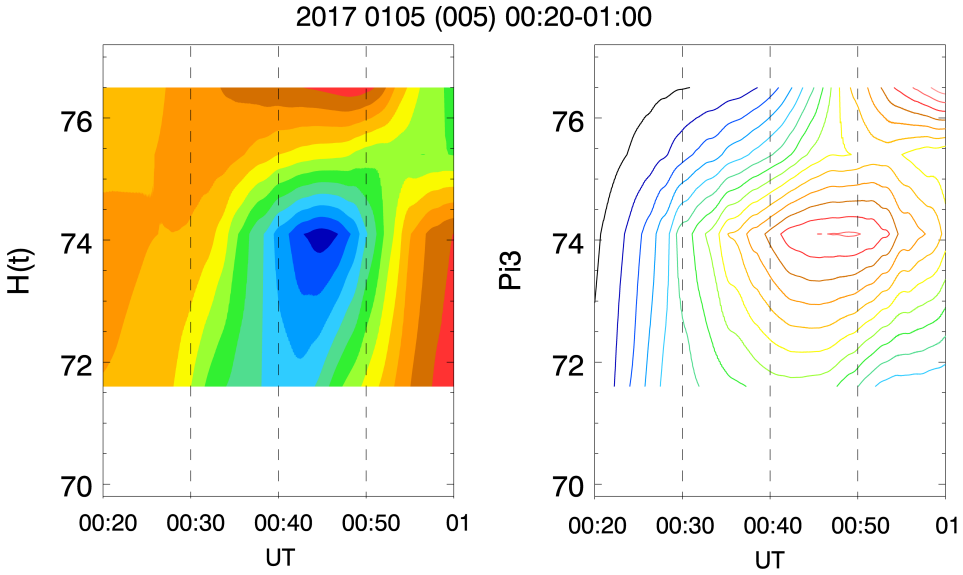

Figure 7: The keograms of ULF power in the band 1.8–2.0 mHz in Northern hemisphere for the event on 2017/01/05, 0020-0100 UT.

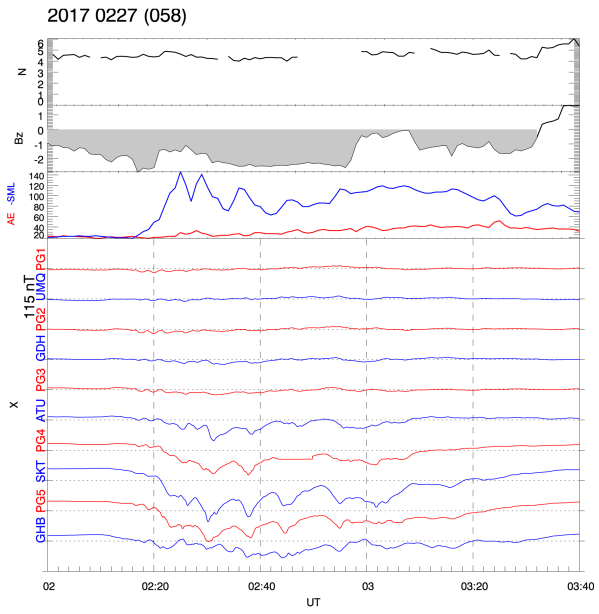

Figure 8: The event on 2017/02/27, 0200-0340 UT, in the same format as in Fig. 2.

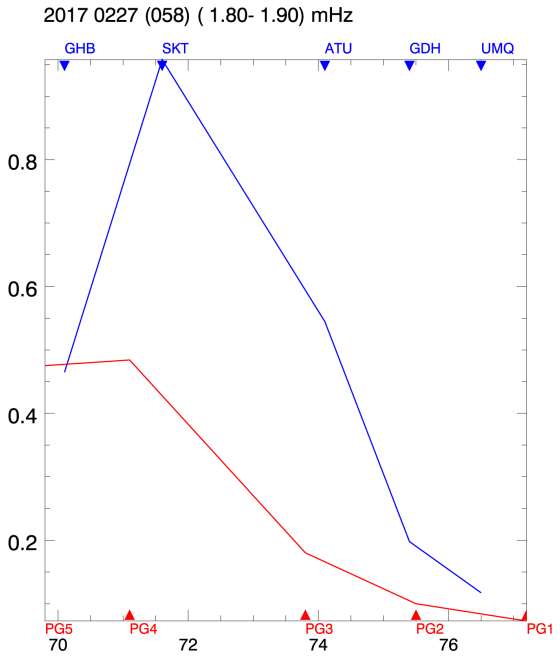

Figure 9: Latitudinal profile of the spectral power in the band 1.8-1.9 mHz in both hemispheres for the event 2017/02/27, 0200-0340 UT.

an intermediate azimuthal wave number m=2–90, were recorded during the expansion phase of a substorm using multiple Super Dual Auroral Radar Network radars [*James et al.*, 2013]. Azimuthally drifting energetic particles associated with the substorms were suggested to be responsible for driving the waves. The pulsation frequency was assumed to be determined by the condition of drift resonance with injected clouds of particles, but not by the local Alfvén period. The adequate theory of Pi3 excitation by plasma instability must be advanced enough to account for characteristic features of these regions – finite plasma pressure, curved magnetic field, plasma and magnetic field inhomogeneity, energetic particle clouds, and wave-particle interactions. Thus, at least some Pi3 pulsations can be the ground counterpart of compressional Pc5–Pc6 pulsations observed by satellites.

A characteristic feature of Pi3 pulsations is that they are accompanied by intense precipitation of electrons strongly modifying the ionospheric conductivity [*Kleimenova et al.*, 2002]. This feature makes them a promising candidate for the feedback ionosphere-magnetosphere instability. This

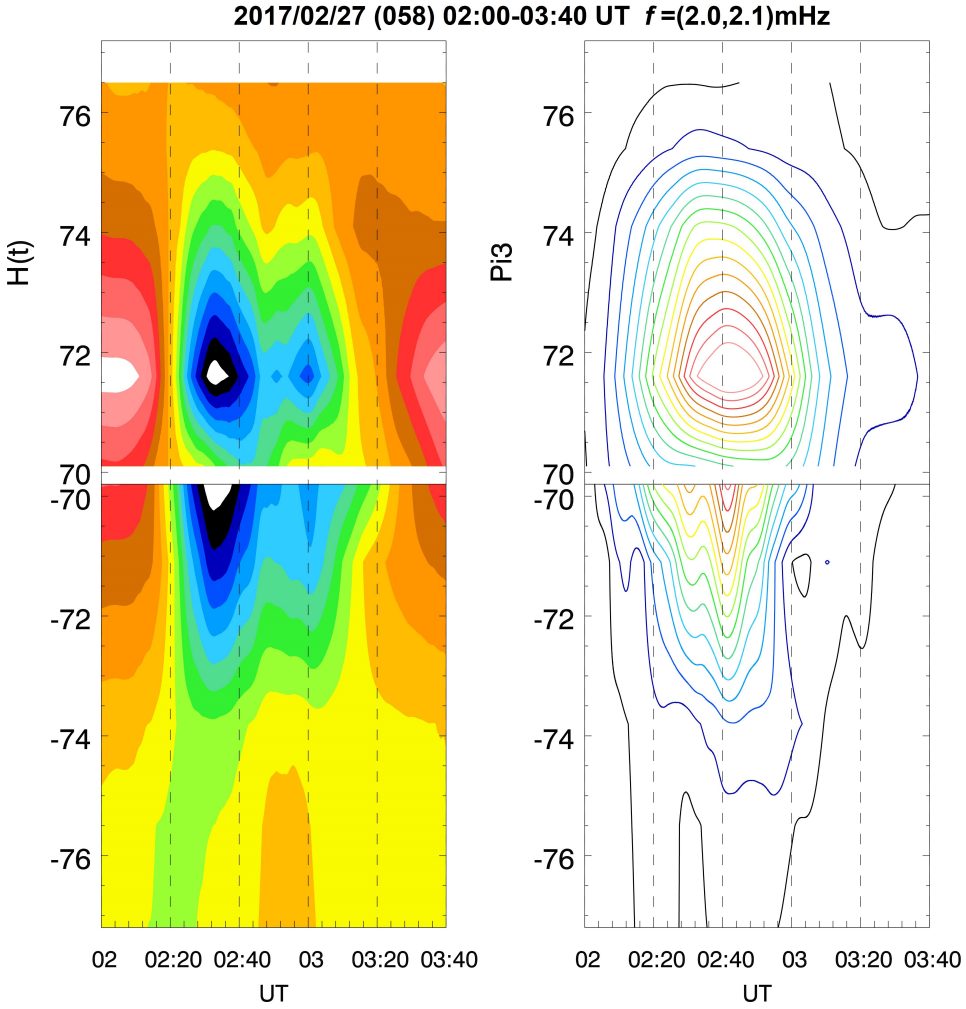

Figure 10: The keogram of the ULF power (in the band 2.0-2.1 mHz) for the event 2017/02/27, 0200-0340 UT. The same format as in Figure 5.

instability is driven by intense ionospheric convection coordinated with periodic modification of the ionospheric conductivity by Alfvén wave modulated precipitation. The feedback instability [*Lysak and Song*, 2002; *Streltsov et al.*, 2010] of the magnetosphere-ionosphere system may lower somewhat the frequencies of unstable Alfvén-type oscillations, but whether the feedback mechanism can shift the frequency of unstable oscillations into the Pi3 band (<2 mHz) was not examined yet.

Another cause of Pi3 periodicity may be quasi-periodic BBF injected from the magnetotail into the nighttime magnetosphere, most actively during substorms. BBF may be quasi-periodic thus producing a periodic response of the nightside magnetosphere. Multi-instrument analysis of substorm event by *Wei et al.* [2021] showed that intense BBF with Earthward velocity ~10^3 km/s at L~6.7 was accompanied by a dipolization front and energetic electron injection. It produced FAC at the low-Earth orbit of ~4 μA/m^2 and magnetic variations on the ground with $|dX/dt|$~400 nT/min. However, the dominant periodicity of the BBF activity is commonly found to be in the range 140–160 s, that is in the Pi2 band, but not in the Pi3 band [*Wu et al.*, 2017]

Pi3 pulsations may be related to a magnetospheric field-line resonator with low Q-factor formed by Alfvénic oscillations of field lines extended far into the magnetotail. This mechanism seemingly should produce a conjugate response in both hemispheres. *Guido et al.* [2014] analyzed frequencies of ULF waves recorded during substorms and demonstrated that the frequency range of the waves carrying most of the power in almost all events was significantly lower, ≤ 1 mHz, than typical Alfvénic oscillations of quasi-dipole field lines at these latitudes. However, the field lines associated with substorm onset strongly deviate from quasi-dipole configuration.

Indeed, in some events, the latitudinal maxima of the ULF power in opposite hemispheres have been observed at non-conjugate pairs of stations. The geomagnetic coordinates and nominal conjugacy between stations are commonly estimated using the internal part of geomagnetic field (e.g.,

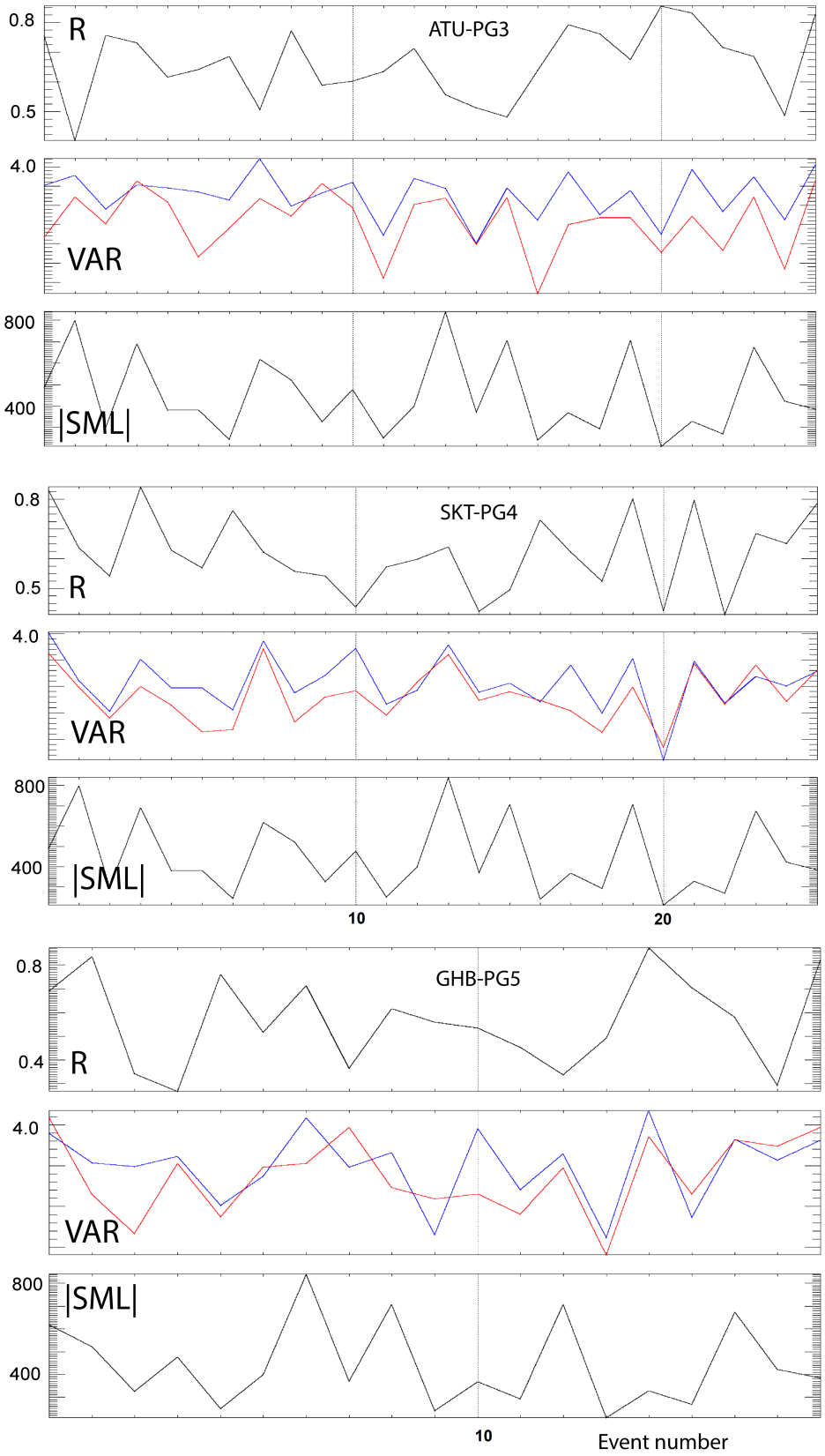

Figure 11: The results of the correlation analysis for 3 pairs of Greenland-Antarctica stations ATU-PG3, SKT-PG4, and GHB-PG5: correlation coefficient R, magnetic field variance VAR at Northern (blue) and Southern (red) stations, and absolute value of SML index.

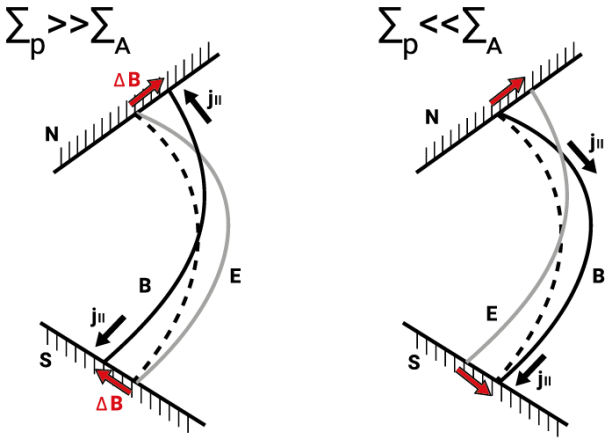

Figure 12: The field-aligned structure of Alfven fundamental mode (electric field $E(s)$, plasma displacement $\xi(s)$, magnetic field $B(s)$, and directions of FAC $j_{||}(s)$ for high conductive ionospheres (left-hand plot) and low-conductive ionosphere (right-hand plot).

IGRF). Magnetospheric disturbances may disturb the magnetic field geometry, but this distortion can be estimated only using some magnetospheric magnetic field model (e.g., Tsyganenko model). We do not know how far this modeling is from reality during substorms. On the other hand, transient field-aligned current (i.e., Alfvenic disturbance) is guided by a real geomagnetic field line. Discrepancy between magnetospheric magnetic field modeling and actual field-aligned propagating Alfvenic disturbance may be the cause that maxima of Pi3 power in opposite hemispheres are observed not at nominal geomagnetically conjugate points.

As schematically illustrated in Figure 13, at high latitudes part of a field line may be strongly extended deep into magnetotail. In the region around the current sheet (dotted area) the magnetic field lines enter a region with a high-β plasma and experience a steep "bending". These factors may result in a substantial reflection of Alfvenic disturbance (i.e., transient FAC) from this region [*Pilipenko et al.*, 2005; *Mager et al.*, 2009] Therefore, the disturbance of FAC driven by some source in one hemisphere, does not penetrate other hemisphere through the region with steep variation of field line curvature. The oscillatory regime may establish on a part of a field line, between the ionosphere and current sheet. Such regime may be responsible for presented above events, when Pi3 pulsations have been observed in one hemisphere only.

The epicenter of Pi3 power has been found to be at the same latitude as the maximal amplitude of magnetic bays. Therefore, the driving mechanism of Pi3 pulsations is to be closely coupled with dynamics of the large-scale magnetosphere-ionosphere system, similar to the model of Pc5 excitation inside the auroral oval [*Pilipenko et al.*, 2016]

Our consideration has shown that Pi3 pulsations may accompany not only substorms, but SMC events as well. Because Pi3 waves are known to be the dominant source of hazardous dB/dt that is potentially damaging to the power grids, one may conclude that SMC, as well as substorms, must be considered as a risky period for the technological systems. In line with this, *Freeman et al.* [2019] deduced that ~14% only of all large dB/dt in the entire data set from mid-latitude magnetometers during substorm expansion/recovery phases were attributable to the substorm current wedge, whereas the remaining perturbations were probably caused by SMC.

Summarizing, we suppose that there are at least two possibilities to comply Alfven mode conception with the Pi3 observations:

- The magnetic field geometry can be far from the dipole-like, e.g. like shown in Fig. 13. As a result, the Alfvenic eigenperiod may be much lower than that expected for a quasi-dipole magnetic field geometry. Moreover, the occurrence of finite-β plasma may additionally modify MHD eigenmodes [*Mazur et al.*, 2014];

- Pi3 pulsations may be associated with Alfven oscillations, though non-resonant, but forced. Then, the quasi-periodic waveform of pulsations is imposed by an unresolved magnetotail driver.

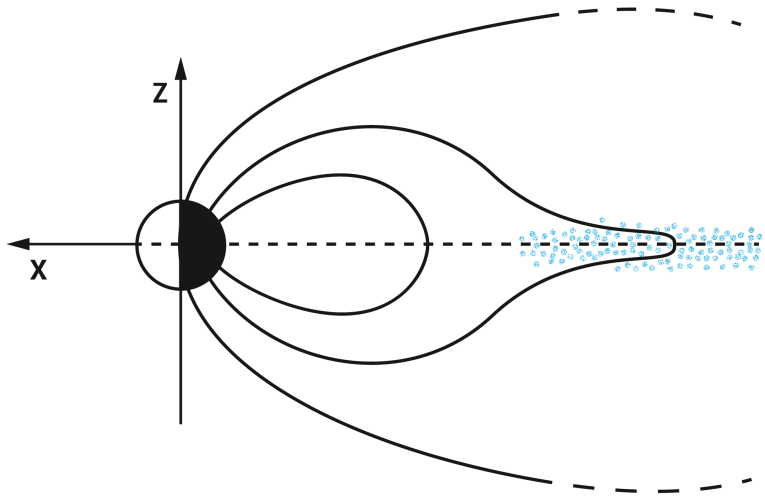

Figure 13: A sketch of the magnetospheric magnetic field geometry at nightside. The field line associated with substorm onset is strongly extended into the magnetotail. In the region around top of this field line a steep variation of field line curvature occurs which results in the Alfven wave reflection.

Conclusion

Evidently, it would be hard to understand the physics of Pi3 pulsations without comprehension of the substorm process itself. Quasi-periodic geomagnetic fluctuations (Pi3 pulsations) accompany both substorm expansion phases and convection bays (SMC events). The epicenter of Pi3 power is found to be at the same latitude as the maximal amplitude of magnetic bays. Therefore, the driving mechanism of Pi3 pulsations is to be closely coupled with dynamics of the large-scale magnetosphere-ionosphere system. The interhemispheric properties of Pi3 pulsations are not consistent: in some events, coherent in-phase magnetic oscillations are observed in both hemispheres, in some – periodic variations are observed in one hemisphere only. The relationships indicate that conjugate Pi3 pulsations must have a field-aligned structure in the magnetosphere with a node of $B(s)$ near the top of a field line. Nonetheless, the found interhemispheric properties of Pi3 pulsations must be taken into consideration by a future theory of this ULF phenomenon.

Acknowledgements. The study is supported by the Russian Science Foundation grant 20-05-00787 (VMB) and grant ES647692 from the program INTPART of Research Council of Norway (NP). The contribution of VP is part of the ISSI project "Understanding Interhemispheric Asymmetry in MIT Coupling". MDH is supported by NSF grants AGS-2027210 and NSF PLR-1744828. Data of the Antarctica-Greenland experiment are available at (http://mist.nianet.org), GOES magnetometer and particle data are provided by NOAA (https://www.ngdc.noaa.gov/stp/satellite/goes/), and OMNI database is available at NASA portal (https://omniweb.gsfc.nasa.gov). The SML index is taken from the SuperMAG portal (https://supermag.jhuapl.edu/indices/). We appreciate the thorough reading and constructive comments of both Reviewers.

References

Buchert, S., G. Haerendel, and W. Baumjohann, A model for the electric fields and currents during a strong ps 6 pulsation event, *Journal of Geophysical Research: Space Physics*, *95*(A4), 3733–3743, doi:https://doi.org/10.1029/JA095iA04p03733, 1990.

Cheng, C.-C., I. R. Mann, and W. Baumjohann, Association of consecutive Pi2-Ps6 band pulsations with earthward fast flows in the plasma sheet in response to IMF variations, *Journal of Geophysical Research: Space Physics*, *119*(5), 3617–3640, doi:10.1002/2013ja019275, 2014.

Clauer, C. R., H. Kim, K. Deshpande, Z. Xu, D. Weimer, S. Musko, G. Crowley, C. Fish, R. Nealy, T. E. Humphreys, J. A. Bhatti, and A. J. Ridley, An autonomous adaptive low-power instrument platform (aal-pip) for remote high-latitude geospace data collection, *Geoscientific Instrumentation, Methods and Data Systems*, *3*(2), 211–227, doi:10.5194/gi-3-211-2014, 2014.

DeJong, A. D., X. Cai, R. C. Clauer, and J. F. Spann, Aurora and open magnetic flux during isolated substorms, sawteeth, and SMC events, *Annales Geophysicae*, *25*(8), 1865–1876, doi:10.5194/angeo-25-1865-2007, 2007.

Freeman, M. P., C. Forsyth, and I. J. Rae, The Influence of Substorms on Extreme Rates of Change of the Surface Horizontal Magnetic Field in the United Kingdom, *Space Weather*, *17*(6), 827–844, doi:10.1029/2018sw002148, 2019.

Guido, T., B. Tulegenov, and A. Streltsov, Large-amplitude ULF waves at high latitudes, *Journal of Atmospheric and Solar-Terrestrial Physics*, *119*, 102-109, doi:10.1016/j.jastp.2014.07.006, 2014.

Han, D.-S., H.-G. Yang, Z.-T. Chen, T. Araki, M. W. Dunlop, M. Nosé, T. Iyemori, Q. Li, Y.-F. Gao, and K. Yumoto, Coupling of perturbations in the solar wind density to global Pi3 pulsations: A case study, *Journal of Geophysical Research: Space Physics*, *112*(A5), A05217, doi:10.1029/2006ja011675, 2007.

James, M. K., T. K. Yeoman, P. N. Mager, and D. Y. Klimushkin, The spatio-temporal characteristics of ULF waves driven by substorm injected particles, *Journal of Geophysical Research: Space Physics*, *118*(4), 1737–1749, doi:10.1002/jgra.50131, 2013.

Keiling, A., Alfvén waves and their roles in the dynamics of the Earth's magnetotail: A review, *Space Science Reviews*, *142*(1-4), 73–156, doi:10.1007/s11214-008-9463-8, 2008.

Kleimenova, N. G., O. V. Kozyreva, K. Kauristie, J. Manninen, and A. Ranta, Case studies on the dynamics of Pi3 geomagnetic and riometer pulsations during auroral activations, *Annales Geophysicae*, *20*(2), 151–159, doi:10.5194/angeo-20-151-2002, 2002.

Kleimenova, N. G., E. E. Antonova, O. V. Kozyreva, L. M. Malysheva, T. A. Kornilova, and I. A. Kornilov, Wave structure of magnetic substorms at high latitudes, *Geomagnetism and Aeronomy*, *52*(6), 746–754, doi:10.1134/S0016793212060059, 2012.

Kozyreva, O. V., V. A. Pilipenko, V. B. Belakhovsky, and Y. A. Sakharov, Ground geomagnetic field and GIC response to March 17, 2015 storm, *Earth, Planets and Space*, *70*(1), 157, doi:10.1186/s40623-018-0933-2, 2018.

Leonovich, A. S., and V. A. Mazur, Why do ultra-low-frequency MHD oscillations with a discrete spectrum exist in the magnetosphere?, *Annales Geophysicae*, *23*(3), 1075–1079, doi:10.5194/angeo-23-1075-2005, 2005.

Lysak, R. L., and Y. Song, Energetics of the ionospheric feedback interaction, *Journal of Geophysical Research: Space Physics*, *107*(A8), SIA 6–1–SIA 6–13, doi:10.1029/2001ja000308, 2002.

Mager, P. N., D. Y. Klimushkin, V. A. Pilipenko, and S. Schäfer, Field-aligned structure of poloidal alfvén waves in a finite pressure plasma, *Annales Geophysicae*, *27*(10), 3875–3882, doi:10.5194/angeo-27-3875-2009, 2009.

Martines-Bedenko, V. A., V. A. Pilipenko, M. J. Engebretson, and M. B. Moldwin, Time-spatial correspondence between pi2 wave power and ultra-violet aurora bursts, *Russian Journal of Earth Sciences*, *17*(4), ES4003, doi:10.2205/2017es000606, 2017.

Mazur, N. G., E. N. Fedorov, and V. A. Pilipenko, Longitudinal structure of ballooning MHD disturbances in a model magnetosphere, *Cosmic Research*, *52*(3), 175–184, doi:10.1134/s0010952514030071, 2014.

Milan, S. E., J. A. Carter, H. Sangha, G. E. Bower, and B. J. Anderson, Magnetospheric Flux Throughput in the Dungey Cycle: Identification of Convection State During 2010, *Journal of Geophysical Research: Space Physics*, *126*(2), e2020JA028437, doi:10.1029/2020ja028437, 2021.

Newell, P. T., and J. W. Gjerloev, Evaluation of SuperMAG auroral electrojet indices as indicators of substorms and auroral power, *Journal of Geophysical Research: Space Physics*, *116*(A12), A12211, doi:10.1029/2011ja016779, 2011.

Partamies, N., T. Pulkkinen, R. McPherron, K. McWilliams, C. Bryant, E. Tanskanen, H. Singer, G. Reeves, and M. Thomsen, Statistical survey on sawtooth events, SMCs and isolated substorms, *Advances in Space Research*, *44*(3), 376–384, doi:10.1016/j.asr.2009.03.013, 2009.

Pilipenko, V., Space weather impact on ground-based technological systems, *Solar-Terrestrial Physics*, *7*(3), 68–104, doi:10.12737/stp-73202106, 2021.

Pilipenko, V. A., N. G. Mazur, E. N. Fedorov, M. J. Engebretson, and D. L. Murr, Alfven wave reflection in a curvilinear magnetic field and formation of Alfvenic resonators on open field lines, *Journal of Geophysical Research: Space Physics*, *110*(A10), A10S05, doi:10.1029/2004JA010755, 2005.

Pilipenko, V. A., D. Y. Klimushkin, P. N. Mager, M. J. Engebretson, and O. V. Kozyreva, Generation of resonant Alfvén waves in the auroral oval, *Annales Geophysicae*, *34*(2), 241–248, doi:10.5194/angeo-34-241-2016, 2016.

Saito, T., Long-period irregular magnetic pulsation, pi3, *Space Science Reviews*, *21*(4), 427-467, doi:10.1007/BF00173068, 1978.

Solovyev, S. I., D. G. Baishev, E. S. Barkova, M. J. Engebretson, J. L. Posch, W. J. Hughes, K. Yumoto, and V. A. Pilipenko, Structure of disturbances in the dayside and nightside ionosphere during periods of negative interplanetary magnetic field Bz, *Journal of Geophysical Research: Space Physics*, *104*(A12), 28019–28039, doi:10.1029/1999ja900286, 1999.

Streltsov, A. V., T. R. Pedersen, E. V. Mishin, and A. L. Snyder, Ionospheric feedback instability and substorm development, *Journal of Geophysical Research: Space Physics*, *115*(A7), A07205, doi:10.1029/2009JA014961, 2010.

Vaivads, A., W. Baumjohann, E. Georgescu, G. Haerendel, R. Nakamura, M. R. Lessard, P. Eglitis, L. M. Kistler, and R. E. Ergun, Correlation studies of compressional Pc5 pulsations in space and Ps6 pulsations on the ground, *Journal of Geophysical Research: Space Physics*, *106*(A12), 29797–29806, doi:10.1029/2001JA900042, 2001.

Wei, D., M. W. Dunlop, J. Yang, X. Dong, Y. Yu, and T. Wang, Intense dB/dt Variations Driven by Near-Earth Bursty Bulk Flows (BBFs): A Case Study, *Geophysical Research Letters*, *48*(4), e2020GL091781, doi:10.1029/2020GL091781, 2021.

Wu, Q., A. M. Du, M. Volwerk, B. T. Tsurutani, and Y. S. Ge, The distribution of oscillation frequency of magnetic field and plasma parameters in bbfs: Themis statistics, *Journal of Geophysical Research: Space Physics*, *122*(4), 4325–4334, doi:10.1002/2016JA023089, 2017.